Frontiers in Heat and Mass Transfer (FHMT), 19, 21 (2022)
DOI: 10.5098/hmt.19.21

Global Digital Central
ISSN: 2151-8629

Frontiers in Heat and Mass Transfer

Available at www.ThermalFluidsCentral.org

THERMAL-HYDRAULIC ANALYSIS OF TRANSIENT CONJUGATE HEATING BETWEEN HEMI-SPHERICAL BODY AND AIR

Farhan Lafta Rashid [a], Abbas Fadhil Khalaf [a], Ahmed Kadhim Hussein [b], Mohamed Bechir Ben Hamida [c,d,e] Bagh Ali [f], Obai Younis [g,*]

[a] *College of Engineering- University of Kerbala –Iraq*
[b] *Mechanical Engineering Department, College of Engineering, University of Babylon, Babylon City, Iraq.*
[c] *College of Engineering, Department of Mechanical Engineering, Imam Mohammad Ibn Saud Islamic University (IMSIU), Riyadh, Saudi Arabia*
[d] *Research Laboratory of Ionized Backgrounds and Reagents Studies (EMIR), Preparatory Institute for Engineering Studies of Monastir (IPEIM), University of Monastir, Monastir City, Tunisia.*
[e] *Higher School of Sciences and Technology of Hammam Sousse (ESSTHS), Department of Physics, University of Sousse, Tunisia.*
[f] *Faculty of Computer Science and Information Technology, Superior University, Lahore 54000, Pakistan*
[g] *Mechanical Engineering Department, College of Engineering inWadiAddwasir, Prince Sattam Bin Abdulaziz University, Alkharj, 11492, KSA.*

ABSTRACT

Convection and conduction in a fluid flow and a rigid body in contact with each other often occur in engineering situations, resulting in unsteady conjugate heat transfer (CHT). Although the analytical solutions to the separate conduction and convection issues are surprisingly straightforward, the combined conjugate heat transfer problem is substantially more complex to solve. This study investigates the CHT of a fluid (air) passing through an unbounded hemisphere. The hemisphere produces heat at a predictable and regular pace. The governing equations are solved using a finite volume system (FVS) using ANSYS Fluent V.16.0, with axisymmetric, no normal convection, and stable physical characteristics assumed. The findings showed The rise in air temperature will result in a more even dispersion of temperature.The temperature distribution will be narrowed as airflow velocity increases. Heat flow increases in the sphere, resulting in a greater temperature gradient over the object's surface.As airflow increases, so does the dispersion of flow rates. Increasing the pace of airflow will lead to an increase in air pressure distribution.

Keywords: *Unsteady conjugate heat transfer, CFD, forced convection, FVM, hemisphere.*

1. INTRODUCTION

It is possible to debate the utility and need for research devoted to conjugating heat transfer from distinct solid entities in laminar crossflow. Convective heat transfer from and to solid substances in many engineering applications is critical. Drying various materials (textiles, veneer, paper, and film materials), cooling glass, plastics, and industrial equipment, such as turbine blades and electronic circuits, are examples of industrial operations where this phenomenon is essential. Other notable uses of this procedure include anemometry and chemical or radioactive contamination/purification.Convection and conduction in a fluid flow and a rigid body in contact with each other often occur in engineering situations, resulting in unsteady conjugate heat transfer (CHT) (Juncu, 2004; Nguyen et al., 1993; Wang et al., 2019). Except for a few fully laminar steady flows (broadband, stochastic, turbulent) (Mathie et al., 2013; Abbas et al., 2020), the vast majority of engineering flows are unstable, either: periodic, which might be 'pulsating' or 'oscillating' (ii) aperiodic; or (iii) quasiperiodic.

Unsteady conjugate heat transmission from or to diverse body geometries has been the focus of a vast number of investigations. Juncu, (1998) investigates two transitory conjugate heat transfer situations in fluid-particle systems. The first relates to a single hard spherical particle at particle Reynolds numbers larger than one. The second is stiff spherical particle assemblages at low particle Reynolds numbers, such as Re 20. The velocity field is considered to be axisymmetric, laminar, and stable. For discretization, finite difference approaches are utilized. The conductivity and heat capacity ratios significantly impact heat transport according to simulation data. Hetsroni et al., (2001) used a Direct Numerical Simulation (DNS) to solve the governing equations for fluid flow and heat transfer around a sphere with nondimensional sphere diameters of 17 and 34 wall units, as well as to cover numerous fluid collocation sites. Using numerical techniques, Gheorghe, (2008) investigated the transient heat transfer from an elliptic cylinder to a continuous viscous, incompressible fluid stream. The cylinder's temperature is thought to be homogeneous in space but not in time. The heat and momentum balance equations were numerically solved in an ecliptic coordinate system. The calculations looked at how the axis and volume heat capacity ratios affected the heat transfer rates. Gheorghe, (2009) investigated conjugate, forced convection mass/heat, and transient transport in multi-particle systems for Reynolds numbers with low to intermediate values using numerical approaches. The momentum and mass/heat balance equations were numerically solved using the finite difference technique in a spherical coordinates system. Reynolds number for the sphere was taken as 100 into account. The calculations estimated

* *Corresponding author email: oubeytaha@hotmail.com*

Global Digital Central
ISSN: 2151-8629

the impact of physical and void characteristics ratios on the mass/heat transfer rate for a sphere with a Peclet number ranging from 10 to 1000.

In an unstable, conjugate way, Gheorghe, (2014) examined forced convection heat transfer from a porous sphere implanted in another porous substance. Fluid has saturated both porous media. The two phases are believed to be in local thermal equilibrium. Outside and inside the sphere, the fluid flow was regarded as incompressible (Darcy and Brinkman flow), axisymmetric, and stable. An implicit alternating direction finite difference approach numerically solved the heat equations in spherical coordinates. For various values of the physical attributes ratios, the impact of Peclet numbers and porous media permeability on the mechanism of heat transmission rate was investigated. In the presence of viscous dissipation, Gheorghe, (2015) investigated the forced convection, unstable, and conjugate heat transfer between a surrounding fluid flow and fluid sphere. Outside and inside the sphere, the fluid flow was described as incompressible, stable, laminar, and axisymmetric. The heat balance equations were numerically solved using a splitting finite difference approach in a spherical coordinates system. For different physical properties ratios, the effect of the Peclet numbers, Reynolds number, and Brinkman on the mechanism of heat transfer rate was investigated. Using a CFD approach based on-house solver, Nanda and Rahul, (2016) examined the phenomena of heat transfer of sphere particles in Newtonian fluids with uniform thermal boundary conditions and velocity slip at the fluid-solid interface. Salleh et al., (2010) considered the boundary layer flow of steady-state mixed convection around a spherical solid produced by Newtonian heating proportional to the local surface temperature.

Also, researchers proposed an empirical equation for the Nusselt numbers of a single sphere with velocity slip as a function of Reynolds and Peclet numbers. The wall temperature and skin friction coefficient, the temperature and velocity profiles, are calculated numerically using many factors, including the mixed convection parameter, the Prandtl number Pr, and the conjugate parameter. Abram and Zachary, (2009) summarized conjugate convective heat transfer issues addressed throughout the current and early stages of this contemporary development. This overview is supplemented by a collection of over 200 papers discussing numerical, complicated and analytical conjugate models for modeling technological, industrial and process equipment ranging from agricultural production to aerospace systems. An investigation of mixed convection around a hot sphere particle traveling vertically downhill in a stagnant fluid column was conducted by Bhattacharyya and Singh, (2008). For the Reynolds number range examined (depending on particle diameter and settling velocity), the fluid flow field is believed to be axisymmetric. The effect of buoyancy on drag and heat transfer rate is investigated. The flow separation is delayed as the sphere's surface temperature rises.

According to literature analysis, despite a great number of studies on unsteady conjugate heat transfer around a hemisphere, the authors are unaware of any previous findings on the issue of assessing conjugate heat transfer in the hemisphere for the laminar fluid flow range. Consequently, this study aims to examine the fluid flow and heat transfer properties in the vicinity of this shape. The impact of several important elements, such as airflow velocity, intake air temperature, and heat flux, will be studied.

2. PROBLEM DESCRIPTION: THE BOUNDARY CONDITIONS AND GOVERNING EQUATIONS

Table 1 and Figure 1 provide the coordinates and dimensions of the case study. The solid sphere has a radius of (R= 2 m) and is surrounded by a rectangular area with dimensions of (6 m x 16 m) that starts 2 m from the right side and wraps around the sphere. The computational space is displayed so that the solution is unaffected by the borders surrounding it. The fluid domain's outside boundaries were left rectangular to make meshing simpler and to achieve low non-orthogonality cells in the fluid domain. The following were used as boundary criteria: The symmetry axis:

- Inlet: $T = T_0, \nabla pn = 0, u = (U, 0, 0), and \tau = 0$
- Outlet : $\nabla Tn = 0, p = 0, \nabla u_i n = 0,\ and\ \nabla \tau_{ij} n = 0$
- The sides of the wedge: The rotational periodicity

Table 1. Coordinates of the studied case

Point no.	1	2	3	4	5	6	7
Angle with x-axis (degree)	0	30	60	90	120	150	180

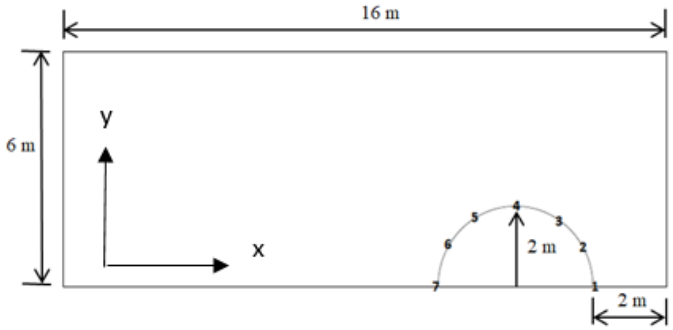

Fig. 1 Coordinates and dimensions of the studied case

3. GOVERNING EQUATIONS

3.1 Fluid region

The equations for momentum balance (Eq. 1) and mass conservation (Eq. 2) are [Eleiwi et al., 2022; Altaie et al., 2014; Rashid et al., 2014; Altaie etal., 2015; Altaie et al., 2015; Altaie et al., 2015]:

$$\rho_f u \nabla u = -\nabla_p + \eta_s \nabla^2 u + \nabla \tau \quad (1)$$

$$\frac{\partial \rho}{\partial t} + \nabla[\rho v] = 0 \quad (2)$$

where:

p: Pressure

u: The vector of velocity

ρ_f: Fluid density

η_s: Solvent viscosity

τ: Polymeric extra-stresses tensor

3.1.2. The constitutive equation

Several constitutive expressions are available for modeling the rheology of viscoelastic fluids (Rashid et al., 2017; Al-Jibory et al., 2018; Al-Jibory et al., 2018).

$$\exp\left(\frac{\varepsilon\lambda}{\eta_p} tr(\tau)\right)\tau + \lambda\tau^{\nabla} = \eta_p(\nabla u + \nabla u^T) \quad (3)$$

Where (ε) is the extensibility factor, (λ) is the fluid duration of relaxation, and (τ^{∇}) *is* the derivative of the upper-convected period (τ).

3.1.3. Energy equation

The energy conservation, as a function of the temperature component, may be defined as (Rashid et al., 2018; Aljibory et al., 2018; Rashid et al., 2018):

$$\rho_f C_{p,f}(u\nabla T) = \nabla\left(k_f \nabla T\right) + \tau' : \nabla u \quad (4)$$

where:

$C_{p,f}$: The fluid specific heat capacity

Global Digital Central
ISSN: 2151-8629

T: The temperature
k_f: The fluid thermal conductivity
It's worth noting that the condition of pure entropy elasticity of the extremely overall term of viscous dissipation corresponds to the term of viscous dissipation ($\tau' : \nabla u$).

3.2. The solid region

3.2.1. Energy equation

In a solid area, that is, inside the sphere, all that is being solved as the energy equation,

$$\nabla(k_s \nabla T) + \Phi = 0 \quad (5)$$

Where: Φ represents the volumetric energy source and $k_s$represents the thermal conductivity of the solid area.

3.2.2. The (solid-fluid) interface

The energy equation computed on each contact side requires close attention to the sphere's surface (Eqns. 4 and 5). The heat flow that spans the surface of a sphere should be comparable on both sides according to the energy conservation equation. Because heat is transferred at the sphere's surface by conduction, the previous condition is (Al-Jibory et al., 2018; AL-Jibory et al., 2020; AL-Jibory et al., 2020):

$$(k_s \nabla T)_{s,i} n_s = \left(-k_f \nabla T\right)_{f,i} n_f \quad (6)$$

In such an overall state, the temperature also complies with the state:

$$(-k_s \nabla T)_{s,i} n_s = h_{res}(T_{s,i} - T_{f,i}) \quad (7)$$

where:
$T_{f,i}$ and $T_{s,i}$Correspondingly, the temperature at the interface on the sides of fluid and solid.
h_{res}: The heat transfer coefficient describes the resistance to contact.

The following assumptions were taken when constructing the model: (1)air flow physical parameters are constant; (2) air flow is incompressible and laminar; and (3) fluid flow and heat transfer unstable states.

3.3 Generation of mesh

Before the governing equations can be solved numerically, a volume grid inside the flow field must be constructed, and the whole boundary surfaces must be discretized. Meshing is the approach used to do this. The meshing consists of (467212) node points derived from cell volumes or, on rare occasions, specified elements (431214). The mesh creation for the scenario is shown in Figure 2.

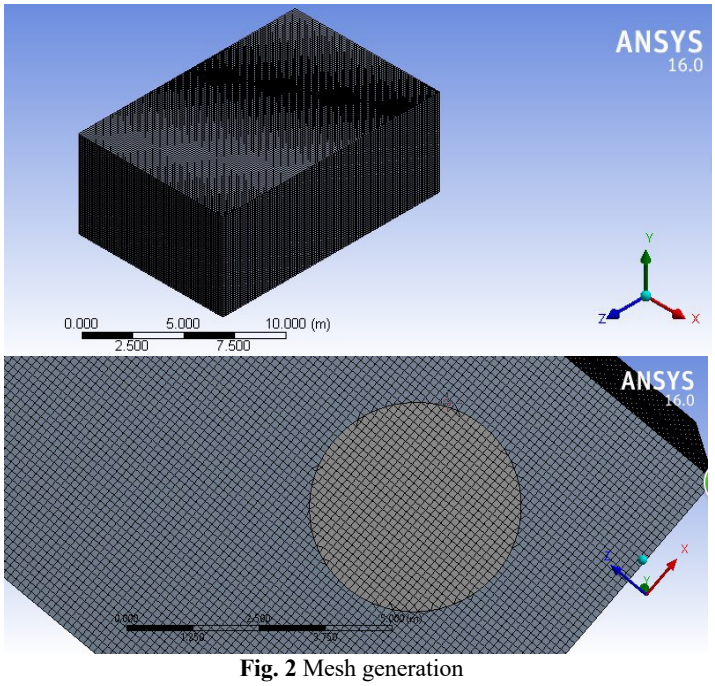

Fig. 2 Mesh generation

3.4 The grid independency study

For the first step of establishing a simulation of the CFD, the mesh size effect on the sensitivity of the result must be examined. More nodes are needed for a more exact technique, and using more nodes will increase the computer's necessary processing memory and time. It is possible to determine the proper nodenumber by enhancing it until the mesh is fine. Figure (3) shows the temperature change as a function of the number of grid cells with a heat flux of (100 W/m^2), input air temperature (293 K), and airflow velocity (0.01 m/s). It was shown that increasing the number of cells boosts the temperature until it reaches a nearly constant value.

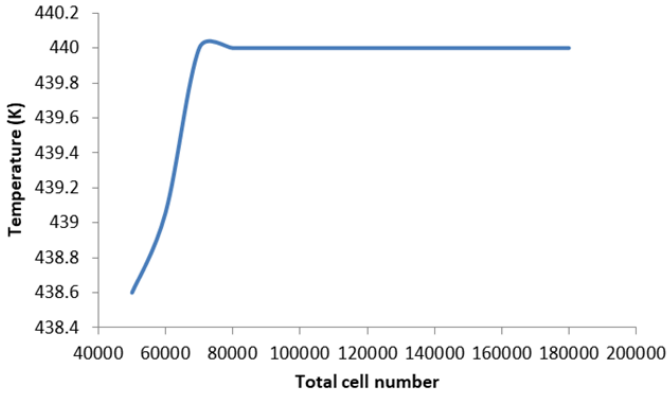

Fig. 3 Study the independency of the grid for the 100 W/m^2 as heat flux, temperature (293 K) of inlet air, and the rate of airflow (0.01 m/s)

4. Results and Discussion

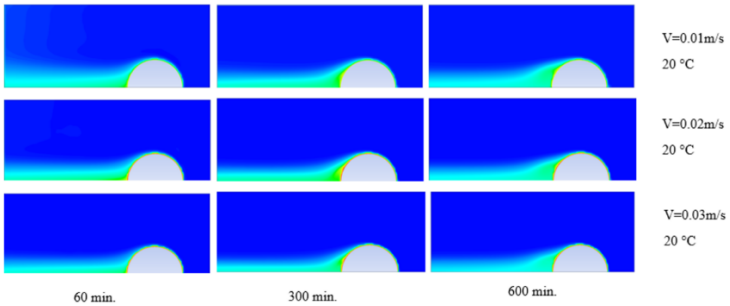

Fig. 4 The contour of temperature distribution along the spherical body for 100 W/m^2 and the inlet air temperature of 293 K, different airflow velocity and time

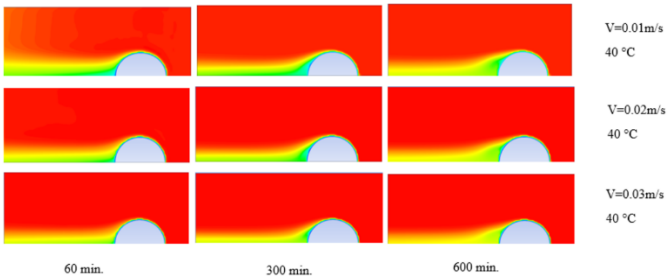

Fig. 5 The contour of temperature distribution along the spherical body for 100 W/m^2 and the inlet air temperature of 313 K, different airflow velocity and time

Figures 4 and 5 show the temperature distribution contour of the airflow case from right to left with three air velocities (0.01, 0.02, 0.03 m/s), a hemisphere body with 100 W/m^2 heat flux, and temperatures of 293, 303, and 313 K, respectively. Depending on the temperature of the coolant air, different temperature contours were seen. Wakes caused by

Global Digital Central
ISSN: 2151-8629

the hemisphere grew into vortices downstream. Because 313 K is higher than the temperature of the hemisphere body, heat transfer from the hemisphere body into the coolant air increased, as shown in figure (4), while heat transfer from the coolant air into the hemisphere decreased, as shown in Figure 5.

Figures 6 and 7 manifest the temperature distribution along with the seventh locations around the hemisphere with varying air velocity and temperature (293, 303, and 313 K, respectively). It also indicates that the temperature climbed at points (1-4), reduced at point 5, raised at point 6, and declined at point 7. This is because the stagnation point will be at point 1 (i.e., the air velocity will be zero), resulting in the least amount of heat transmission. The airflow will rise at points 2, 3, and 4, increasing heat transfer. As illustrated in figures (9), the airflow velocity seems to be at its highest at point 5. As a result, the most heat transfer will occur at this location, resulting in the lowest temperature. At points 6 and 7, the scenario will be replayed.

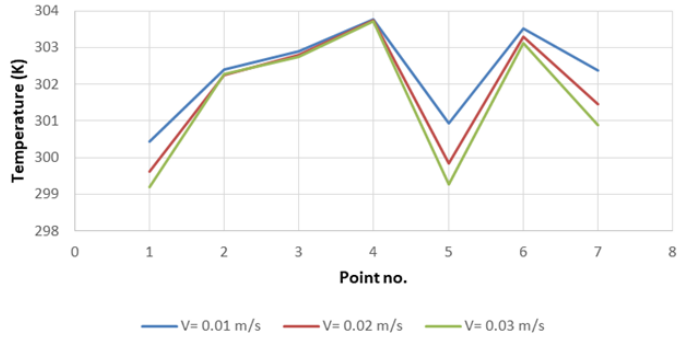

Fig. 6 Temperature distribution along the spherical body for 100 W/m^2 and the inlet air temperature of 293 K, different airflow velocity at 300 min.

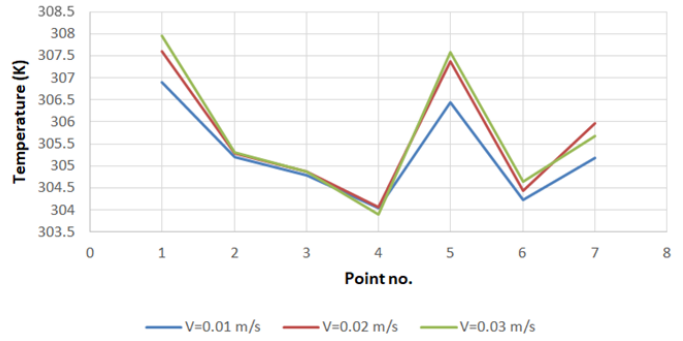

Fig. 7 Temperature distribution along the spherical body for 100 W/m^2 and the inlet air temperature of 313 K, different airflow velocities at 300 min.

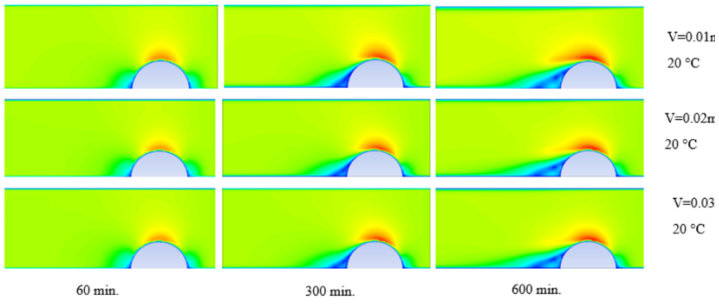

Fig. 8 The contour of velocity distribution along the spherical body for 100 W/m^2 and the inlet air temperature of 293 K, different airflow velocity and time

Figure 8 illustrates the contour of the airflow case from right to left with three air velocities (0.01, 0.02, 0.03 m/s), a hemisphere body with 100 W/m^2 as heat flux, and temperatures of 293 K. Three air velocities (0.01, 0.02, and 0.03 m/s), a hemisphere body with 100 W/m^2 as heat flux, and temperatures of 293 K, are shown in Figure 10.

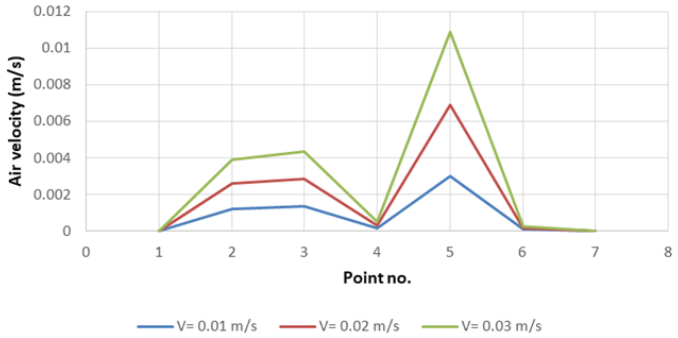

Fig. 9 Velocity distribution along the spherical body for 100 W/m^2 and the inlet air temperature of 293 K, different airflow velocities at 300 min.

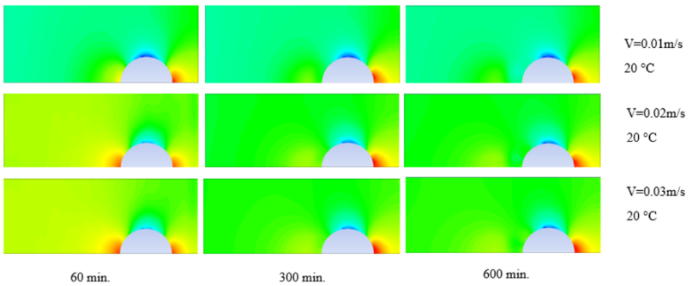

Fig. 10 The contour of pressure distribution along the spherical body for 100 W/m^2 and the inlet air temperature of 293 K, different airflow velocity and time

As seen in Figure 11, seven places around the sphere's circumference are subjected to pressure. The pressure distribution over the two sides of the sphere may be semi-symmetric, with the largest value at point 1 and the least value at point 4 (vacuum). While the pressure value at point 7 is almost identical to that at point 1 (within 0.01 m/s), the opposite sign is present. These graphs show that pressure distribution is unaffected by temperature increases in the air.

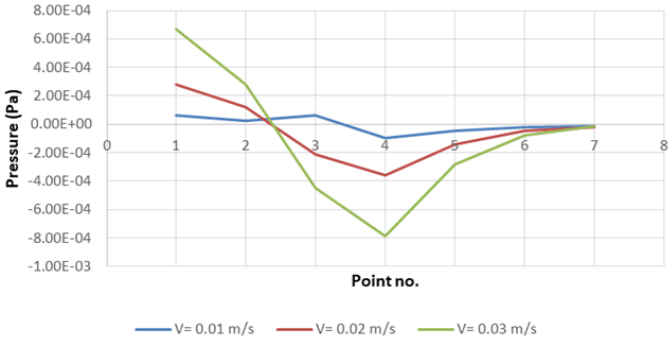

Fig. 11 Pressure distribution along the spherical body for 100 W/m^2 and the inlet air temperature of 293 K, different airflow velocities at 300 min.

To demonstrate the temperature distribution along with the seventh point with an air velocity of 0.03 m/s and varied air temperatures, Figure 12 shows two scenarios with different heat fluxes (100 and 200 W/m). The

highest temperature distribution occurs at 313 K and a heat flux of 200 W/m^2, while the lowest occurs at 293 K and 100 W/m^2 as heat flux.

At point (5), input air temperature of 313 K, heat flux (100 W/m^2), and flow velocity of (0.01, 0.02, and 0.03 m/s) are shown in Figure (13) as the temperature distribution changes over time under these conditions. It is clear that the temperature will rise over time due to heat transmission. Figure (14) depicts the heat transfer coefficient at the seventh point in distinct locations across the hemisphere using different airflow velocities. The increase in airflow velocity increases the heat transfer coefficient, as can be seen from this. It's because points (3, 5) have the greatest airflow rates, while point (4) has the lowest, that the maximum value of heat transfer coefficient happens at points (3, 5), while the least value took place at point (4).

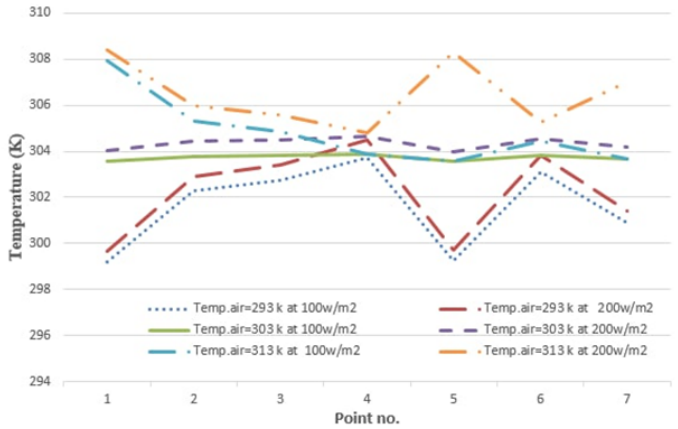

Fig. 12 Temperature variation along the spherical body (100 W/m^2 and 200 W/m^2) at an airflow velocity of 0.03 m/s with different inlet air temperature

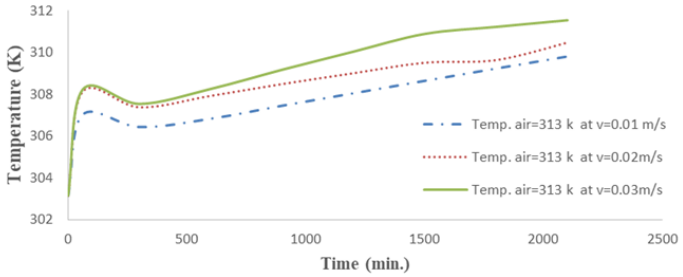

Fig. 13 Temperature distribution at point no. (5) on the spherical body (with 100 W/m^2) with time at different airflow velocity and inlet air temperature of 313 K

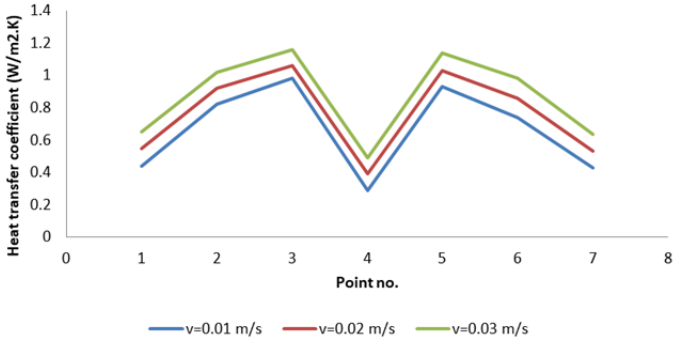

Fig. 14 Heat transfer coefficient along the spherical body for an inlet air temperature (293 K) with different airflow velocities at 300 min.

4. CONCLUSIONS

Unsteady state conditions were used to study heat transfer and the limitless flow of an aerodynamically-smoothed air fluid. The sphere's interior generates an even and constant flow of thermal energy. The convective CHT's difficulties are now being simulated in several disciplines using advanced simulations. For the first time since it was introduced in the late 1960s and early 1970s to model simple processes, this method is now being used for more complex multistage non-linear processes, such as those found in information technology (IT). Next, we arrive at a list of possible outcomes:

- The rise in air temperature will result in a more even dispersion of temperature.
- The temperature distribution will be narrowed as airflow velocity increases.
- Heat flow increases in the sphere, resulting in a greater temperature gradient over the object's surface.
- As airflow increases, so does the dispersion of flow rates.
- Increasing the pace of airflow will lead to an increase in air pressure distribution.

ACKNOWLEDGMENTS

This publication was supported by the Deanship of Scientific Research at Prince Sattam bin Abdulaziz University, Alkharj, Saudi Arabia.

NOMENCLATURE

$C_{p,f}$	The fluid specific heat capacity (Kj/kg.K)
h	Heat transfer coefficient (W/m^{2}K)
k_f	The fluid thermal conductivity(W/mK)
k_s	The thermal conductivity of the solid area(W/mK)
P	Pressure (Pa)
T	The temperature (K)
U	The vector of velocity (-)

Greek Symbols

ε	The extensibility factor (-)
λ	The fluid duration of relaxation (-)
ρ_f	Fluid density (kg/m^3)
η_s	Solvent viscosity (Pa.s)
τ	Polymeric extra-stresses tensor (-)
τ^{∇}	The derivative of the upper-convected period (τ)
Φ	The volumetric energy source (-)

REFERENCES

Juncu, Gh., 2004, "Unsteady conjugate heat/mass transfer from a circular cylinder in laminar crossflow at low Reynolds numbers", International Journal of Heat and Mass Transfer, 47(10–11), 2469-2480.https://doi.org/10.1016/j.ijheatmasstransfer.2003.10.035

Nguyen, H.D, Paik, E., and Chung, J.N.,1993,"Unsteady mixed convection heat transfer from a solid sphere: the conjugate problem", Int. J. Heat Mass Transfer, 36(18), 4443-4453.

Wang, L., Zhao, Y., Yang, X., Shi, B., and Chai, Z., 2019, " A lattice Boltzmann analysis of the conjugate natural convection in a square enclosure with a circular cylinder", Applied Mathematical Modelling, 71, 31-44.https://doi.org/10.1016/j.apm.2019.02.012

Mathie, R., Nakamura, H., and Markides, C.N., 2013," Heat transfer augmentation in unsteady conjugate thermal systems – Part II: Applications", International Journal of Heat and Mass Transfer, 56(1–2), 819-833. https://doi.org/10.1016/j.ijheatmasstransfer.2012.09.017

Abbas, A., Ashraf, M., Chu, Y-M., Zia, S., Khan, I., and Nisar, K.S., 2020, "Computational Study of the Coupled Mechanism of

Thermophoretic Transportation and Mixed Convection Flow around the Surface of a Sphere", Molecules 25(11), 2694. https://doi.org/10.3390/molecules25112694

Juncu, Gh., 1998,"Unsteady conjugate heat transfer for a single particle and in multi-particle systems at low Reynolds numbers", Int. J. Heat Mass Transfer, 41(3), 529-536.

Hetsroni, G., Li, C.F., Mosyak, A., and Tiselj, I., 2001, " Heat Transfer and Thermal Patterns around a sphere in Turbulent Boundary Layer", International Journal of Multiphase Flow, 27, 1127-1150.

Juncu, Gh., 2008, "Unsteady heat transfer from an elliptic cylinder", International Journal of Heat and Mass Transfer, 51(3–4), 920-928. https://doi.org/10.1016/j.ijheatmasstransfer.2007.11.001

Juncu, Gh., 2009, "Unsteady conjugate forced convection heat/mass transfer in ensembles of spherical particles with cell models", International Journal of Heat and Mass Transfer, 52(7–8), 1817-1826. https://doi.org/10.1016/j.ijheatmasstransfer.2008.10.010

Juncu, Gh., 2014," The influence of the porous media permeability on the unsteady conjugate forced convection heat transfer from a porous sphere embedded in a porous medium", International Journal of Heat and Mass Transfer, 77, 1124-1132. https://doi.org/10.1016/j.ijheatmasstransfer.2014.06.039

Juncu, Gh., 2015, "The influence of viscous dissipation on the unsteady conjugate forced convection heat transfer from a fluid sphere", International Journal of Heat and Mass Transfer, 90, 542-551. https://doi.org/10.1016/j.ijheatmasstransfer.2015.07.010

Kishore, N., and Ramteke, R.R., 2016, "Forced convective heat transfer from spheres to Newtonian fluids in steady axisymmetric flow regime with velocity slip at the fluid-solid interface", International Journal of Thermal Sciences, 105, 206-217. https://doi.org/10.1016/j.ijthermalsci.2016.03.009

Salleh,V, Nazar, R., and Pop, I., 2010, "Mixed convection boundary layer flow about a solid sphere with Newtonian heating", Arch. Mech., 62(4), 283–303.

Dorfman, A., and Renner, Z., 2009, "Conjugate Problems in Convective Heat Transfer: Review", Mathematical Problems in Engineering, 927350, 1-27. https://doi.org/10.1155/2009/927350

Bhattacharyya, S., and Singh, A., 2008, " Mixed Convection from an isolated spherical particle", International Journal of Heat and Mass Transfer 51, 1034–1048. https://doi.org/10.1016/j.ijheatmasstransfer.2007.05.033

Eleiwi, M.A., Rashid, F.L., Khalaf, A.F., and Tuama, S.A., 2022, " Numerical Investigation of Conjugate Heat Transfer between Spherical Solid-Body and Fluid", Mathematical Modelling of Engineering Problems, 9(2).

Altaie, A., Hasan, M.R., and Rashid, F.L., 2014," Numerical Heat Transfer and Turbulent Flow in a Circular Tube Fitted with Opened Rings Having Square Cross Section", Journal of Basic and Applied Scientific Research, 4(11), 28-36.

Rashid, F.L., Altaie, A., and Hasan, M.R., 2014, " Numerical Investigation of Heat Transfer Enhancement in a Circular Tube Using Ribs of Separated Ports Assembly", European Scientific Journal.

Altaie, A., Hasan, M.R., and Rashid, F.L., 2015, " Numerical Investigation of Heat Transfer Enhancement in a Circular Tube with Rectangular Opened Rings", Bulletin of Electrical Engineering and Informatics, 4(1), 18-25.

Altaie, A., Hasan,M.R., and Rashid, F.L., 2015," Heat Transfer Enhancement in a Circular Tube Using Ribs with Middle Arm", Elixir International Journal.

Altaie, A., Hasan, M.R., and Rashid, F.L., 2015, " Numerical Investigation in a Circular Tube to Enhance Turbulent Heat Transfer Using Opened Rings-Triangular Cross Section", Journal of Babylon University/ Engineering Sciences.

Rashid, F.L., Al-Jibory, M.W., and Hussein, H.Q., 2017, " Cooling Enhancement in Gas Turbine Blade Using Coated Circular Ribs with a New Nanocomposite Material", Patent (5092).

Al-Jibory, M.W., Rashid, F.L., and Hussein, H.Q., 2018, " Heat Transfer Augmentation in Gas Turbine Blade Rectangular Passages Using Circular Ribs with Fins", Journal of University of Babylon, Engineering Sciences, 26(1), 247-258.

Al-Jibory, M.W., Rashid, F.L., and Talib, S.M., 2018," Numerical Investigation of Heat Transfer Enhancement in Ribbed Elliptical Passage", Journal of Engineering and Applied Sciences, 13(17), 7223-7234.

Rashid, F.L., Azziz, H.N., and Hussein, E.Q., 2018," Heat Transfer Enhancement in Air-Cooled Gas Turbine Blade Using Corrugated Passages", Journal of Petroleum Research & Studies, 20, 52-69.

Aljibory, M.W., Rashid, F.L, and Alais, Sh.M., 2018, "An Experimental and numerical investigation of heat transfer enhancement using annular ribs in a tube", IOP Conference Series: Materials Science and Engineering, 433(1), 012057.

Rashid, F.L., Al-Jibory, M.W., and Talib, Sh.M., 2018, "Numerical Investigation of Heat Transfer Augmentation in Elliptical Passage with Different rib Geometries and Aspect Ratios", International Journal of Mechanical Engineering and Technology, 9(13), 1390-1409.

Al-Jibory, M.W., Rashid, F.L., and Talib, Sh.M., 2018, "An Experimental Investigation of Heat Transfer Enhancement in Elliptical Passage Fitted with Different rib Geometries", International Journal of Mechanical Engineering and Technology, 9(13), 1033-1048.

AL-Jibory, M.W., Rashid, F.L., and Talib, Sh.M., 2020, "Review on Cooling Enhancement of Different Shape Gas Turbine Ribbed Blade with Thermal Barrier Coating", International Journal of Scientific Research and Engineering Development, 3(1), 313-329.

AL-Jibory, M.W., Rashid, F.L., and Hussein, H.Q., 2020, "Review of Heat Transfer Enhancement in Air-Cooled Turbine Blades", International Journal of Scientific & Technology Research, 9(4), 3123-3130.